

# An Antibody Binding Site on Cytochrome c Defined by Hydrogen Exchange and Two-Dimensional NMR

YVONNE PATERSON, S. WALTER ENGLANDER, HEINRICH RODER

The interaction of a protein antigen, horse cytochrome c (cyt c), with a monoclonal antibody has been studied by hydrogen-deuterium (H-D) exchange labeling and two-dimensional nuclear magnetic resonance (2D NMR) methods. The H-exchange rate of residues in three discontinuous regions of the cyt c polypeptide backbone was slowed by factors up to 340-fold in the antibody-antigen complex compared with free cyt c. The protected residues, 36 to 38, 59, 60, 64 to 67, 100, and 101, and their hydrogen-bond acceptors, are brought together in the three-dimensional structure to form a contiguous, largely exposed protein surface with an area of about 750 square angstroms. The interaction site determined in this way is consistent with prior epitope mapping studies and includes several residues that were not previously identified. The hydrogen exchange labeling approach can be used to map binding sites on small proteins in antibody-antigen complexes and may be applicable to protein-protein and protein-ligand interactions in general.

PROTEIN-PROTEIN INTERACTIONS ARE OFTEN CHARACTERIZED by highly specific surface contacts, as is the case for the interaction between a protein antigen and the antibody combining site. A complete structural description of an antibody-protein interaction surface has been obtained in a few cases by x-ray diffraction (1, 2). In most cases, other, less specific methods for three-dimensional epitope mapping have been used to determine which residues are involved, and include the use of protein analogs that differ from the antigen by a limited number of defined mutational or chemical modifications (3-5) and the immunoprotection of the antigenic surface against proteolysis or chemical modification (6, 7). When used together, these approaches can identify the general region of the protein antigen to which the antibody binds but give only an incomplete view of the epitopic surface (8).

Recent progress in 2D NMR spectroscopy (9) has made it possible to obtain complete proton resonance assignments for small proteins and to determine their structure in solution [reviewed

recently (10)]. However, 2D NMR spectroscopy is at present not applicable to large antibody-protein complexes. Thus previous NMR studies have been limited to examining the interaction of small molecules with antibodies. These studies include 1D and 2D magnetization transfer and transferred nuclear Overhauser effect experiments on complexes of antibodies to hapten (11) and peptide (12) that were directed at defining individual aromatic residues in the combining site of the antibody and  $^{31}\text{P}$  and  $^{19}\text{F}$  NMR studies of the kinetics of hapten binding to antibodies (13).

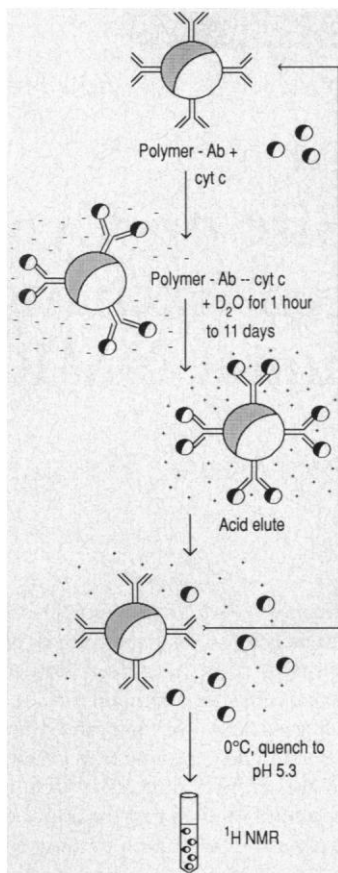
The method used here to study the binding of horse cyt c to a monoclonal antibody (MAb) combines the immunoprotection of the antigen by the antibody with hydrogen exchange labeling and 2D  $^1\text{H}$  NMR analysis. This method provides a facile approach for mapping antigenic sites on small proteins almost to the resolution of single amino acid residues and appears applicable to protein-protein and protein-nucleic acid interactions in general. Horse cyt c is a structurally well-characterized protein of 104 residues (14, 15). Its  $^1\text{H}$  NMR resonances in both oxidation states have been assigned by 2D NMR studies (16). The MAb E8 is specific for horse cyt c and binds with high affinity (dissociation constant,  $K_d \approx 10^{-9}$  M) (17). Previous epitope mapping techniques (4-6, 8) have so far defined four E8-specific antigenic site residues on one surface of cyt c, Trp<sup>59</sup>, Lys<sup>60</sup>, Glu<sup>66</sup>, and Lys<sup>99</sup>.

**Hydrogen exchange of antibody-bound cyt c.** THE H-D exchange reaction was initiated by transferring the immobilized antibody-antigen complex from  $\text{H}_2\text{O}$  into  $\text{D}_2\text{O}$  (Fig. 1). After various H-D exchange time periods, the complex was dissociated under slow H-exchange conditions, the antigen was isolated, and the remaining hydrogen label on individual amide sites was determined by 2D NMR analysis. The effect of antibody binding on the exchange kinetics of amide hydrogens on the antigen can thus be measured. The H-exchange procedure was greatly facilitated by immobilizing the antibody on a solid support, which allowed for rapid re-isolation of the exchange-labeled antigen and re-use of the antibody for subsequent time points. Because cyt c is available commercially, we used a new sample of antigen for each experiment, but the protein could be recovered after NMR data collection, re-exchanged in  $\text{H}_2\text{O}$ , and used again.

Representative contour plots of the NH- $\text{C}\alpha\text{H}$  cross-peak region in 2D COSY ( $J$ -correlated spectroscopy) spectra of cyt c are shown in Fig. 2 (left panels). For comparison, 2D NMR spectra from earlier H-exchange experiments on free oxidized cyt c (18), performed under the same conditions (20°C, pD 7) and at similar exchange times, are also shown (right panels).

Y. Paterson is in the Department of Microbiology and S. W. Englander and H. Roder are in the Department of Biochemistry and Biophysics, University of Pennsylvania, Philadelphia, PA 19104.

**Fig. 1.** Procedure for hydrogen exchange on antibody-bound cyt c. Affinity-purified MAb E8 (17) (100 mg) was coupled to 12 ml (packed gel volume) of Affigel 10 (Bio-Rad) according to the manufacturers instructions. The polymer-bound antibody was incubated with 25 mg of oxidized horse cyt c (Sigma, Type VI) in 50 mM  $\text{KH}_2/\text{K}_2\text{HPO}_4$  buffer (pH 7.0) for 2 hours at room temperature with gentle rocking and was then transferred to a column (1.5 cm by 30 cm). Unbound cyt c was removed by washing copiously with potassium phosphate buffer to leave ~11 mg of antigen bound to E8. To initiate exchange, the column was washed into  $\text{D}_2\text{O}$  (50 mM  $\text{KH}_2/\text{K}_2\text{HPO}_4$  at pD 7.0) and incubated at 20°C for time intervals ranging from 1 hour to 11 days in a series of H-D exchange experiments. Subsequent manipulations, designed to re-isolate cyt c while minimizing further H-D exchange, were performed at 8°C. The column was washed with  $\text{D}_2\text{O}$  with low buffer capacity (1 mM  $\text{KH}_2/\text{K}_2\text{HPO}_4$  at pD 6.0), and cyt c was then eluted in a minimal volume of 0.2 M acetic acid, 1 M NaCl at pD 2.5. Fractions (1-ml volume) were collected into 0.3 ml of cold 0.5 M  $\text{KH}_2/\text{K}_2\text{HPO}_4$  buffer at pD 7.5 containing 40 mM ascorbic acid to reduce cyt c and produce a final pD of ~5.3. The fractions were pooled and concentrated on an Amicon filter (YM5) to 400  $\mu\text{l}$  for NMR analysis (1.5 to 2 mM cyt c). These procedures were carried out at seven different hydrogen-exchange incubation times (1, 3, 8, 9, 26, 92, and 266 hours).



The effect of antibody binding on H-exchange can be seen by comparing the peak intensities for corresponding amide protons in the free and the bound form for each time point (Fig. 2). Differences are most dramatic at the longest exchange time (11 days). In free cyt c only the amides of residues 10, 32, and 94 to 98 still give rise to measurable cross peaks in sections of 2D NMR spectra shown in Fig. 2. In the spectra for antibody-bound cyt c, cross peaks are also apparent for residues 12, 36, 38, 59, 60, 64, 65, 69, 100, and 101.

The COSY spectrum of oxidized cyt c freshly dissolved in  $\text{D}_2\text{O}$  reveals 41 NH-C $\alpha$ H cross peaks with sufficient resolution, intensity, and H-exchange lifetime to support accurate H-exchange measurements. After 1 month of exchange in the free form, eight of these NH groups remained unexchanged and could not serve as probes for the further slowing of H-exchange in the complex at the pH and temperature used in these studies (pH 7.0 and 20°C). The H-D exchange rates for the 33 amide protons that did show significant exchange in this time period were obtained by plotting the decreasing intensity of each NH-C $\alpha$ H cross peak against time of exchange in  $\text{D}_2\text{O}$  (examples are shown in Fig. 3). For some protons, the amplitude of the NH resonances resolved in the 1D NMR spectrum were used.

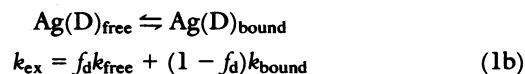
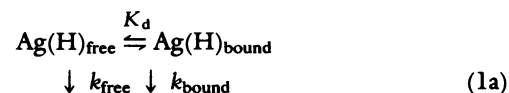
Exchange rates in free cyt c ( $k_{\text{free}}$ ) and in the cyt c-antibody complex ( $k_{\text{bound}}$ ) for residues with protection factors ( $k_{\text{free}}/k_{\text{bound}}$ ) greater than 3 are listed in Table 1. For these sites, antibody binding dramatically reduced H-exchange rates, with protection factors ranging from 7- up to 340-fold. Five amide protons with measurable exchange rates in the free form remained unexchanged in the antibody complex out to the longest exchange time measured (for

example, Lys<sup>60</sup> and Leu<sup>64</sup> in Fig. 3). For these cases one can only obtain a lower limit for the protection factor (Table 1).

**Hydrogen exchange mechanism and protein-protein interaction.** The kinetics of exchange between protein and solvent hydrogens are sensitive to subtle conformational changes (18, 19) and have found extensive use in the study of dynamic aspects of protein structure [reviewed in (20)] and ligand receptor binding (21). It is generally accepted that hydrogen exchange from native proteins is mediated by internal motions of the protein structure, although various models have been proposed that differ in the detailed nature of these fluctuations (20). The structural unfolding model (22) suggests that slowly exchanging protein hydrogens are those that form intramolecular hydrogen bonds, that the exchange process involves the transient breaking of hydrogen bonds, and that hydrogen-bond breaking tends to occur in locally cooperative segmental-unfolding reactions. In alternative models for protein hydrogen exchange, the slowly exchanging protein hydrogens are in some sense buried, and their exchange depends on some kind of penetration process in which the hydrogen-exchange catalyst,  $\text{OH}^-$  in the present experiments, enters the protein and directly catalyzes exchange of the buried hydrogens (23).

The great majority of slowly exchanging protein hydrogens are in fact involved in H-bonds, and locally cooperative hydrogen-exchange can occur in individual helical segments of a number of proteins (18, 24). For this discussion, we adopt the local unfolding point of view, although most of the conclusions reached stand outside of this assumption. Either model would predict that labile hydrogens at or near the surface protected in a protein-protein complex should exhibit slowed exchange.

The degree of protection against hydrogen exchange achieved in the complex can be considered in the context of reaction scheme 1.



Any labile hydrogen in the antigen [ $\text{Ag(H)}$ ] exchanges with  $\text{D}_2\text{O}$  at its normal rate ( $k_{\text{free}}$ ) from the equilibrium fraction of dissociated antigen ( $f_d$ ), and may exchange at an altered rate ( $k_{\text{bound}}$ ) from the antibody-bound antigen (Eq. 1a). In most cases antibody binding and dissociation rates are fast compared to H-exchange rates, so that the measured rate ( $k_{\text{ex}}$ ) is the weighted sum of these two terms (Eq. 1b). The rate constant,  $k_{\text{ex}}$ , can range from  $k_{\text{free}}$  for unaffected protons (when  $k_{\text{bound}} = k_{\text{free}}$ ) to a minimum rate of  $f_d k_{\text{free}}$  when the exchange rate in the complex is exceedingly small. When the exchange rate is accelerated in the complex, for example because of some structural destabilization, the maximum rate can range to  $(1 - f_d) k_{\text{bound}}$ . In the present case, the primary effect of complex formation is to slow exchange (Table 1).

The present experiments deal with a high-affinity, stoichiometric complex where all available antibody binding sites are saturated with antigen. Therefore  $f_d$  can be expressed in terms of the equilibrium dissociation constant,  $K_d$ , and the concentration of antigen-antibody complex,  $[\text{Ag} \cdot \text{Ab}]$ , as in Eq. 2 (derived from the simple binding equation with  $[\text{Ag}]_{\text{free}} = [\text{Ab}]_{\text{free}}$ ).

$$f_d = (K_d/[\text{Ag} \cdot \text{Ab}])^{1/2} \quad (2)$$

The slowest exchange rate,  $k_{\text{ex,min}}$ , given by Eq. 3, occurs when  $k_{\text{bound}}$  is  $\sim 0$ .

$$k_{\text{ex,min}} = f_d k_{\text{free}} = k_{\text{free}} (K_d/[\text{Ag} \cdot \text{Ab}])^{1/2} \quad (3)$$

The largest possible protection factor due to antibody-induced retardation of exchange, then, is

$$k_{\text{free}}/k_{\text{ex,min}} = 1/f_d = ([\text{Ag} \cdot \text{Ab}]/K_d)^{1/2} \quad (4)$$

For the cyt c-E8 complex,  $K_d \approx 10^{-9}$  M, and  $[\text{Ag} \cdot \text{Ab}]$  in the available volume of the affinity column is  $\sim 10^{-4}$  M ( $\sim 1/3$  of total column bed volume). Thus the largest possible value of  $1/f_d$  for this system is  $\sim 300$ , close to the largest protection factors measured in this study (Table 1). These calculations indicate that the most strongly retarded amide protons, on residues 38, 59, 100, and 101, and possibly five others (36, 37, 60, 64, and 65), do not exchange from within the antigen-antibody complex, but require prior equilibrium dissociation of the complex. The large slowing factors observed suggest that surfaces of the antigen and antibody fit together in fairly intimate contact over this region.

**Definition of the cyt c epitope for E8 by hydrogen exchange labeling.** The results in Table 1 show that a majority of the exchangeable hydrogens were little affected in the antibody complex (protection factors  $\leq 3$ ), indicating that the overall structure of cyt c and the stability of regions outside the binding site were hardly perturbed by the interaction with E8. In contrast, 12 residues underwent a 7- to 340-fold reduction in H-exchange rate on binding to the E8 MAb. As illustrated in Fig. 4A, these slowed NH and their hydrogen-bonded acceptors (Gln<sup>12</sup> excluded) are clustered into three short segments of the polypeptide backbone, residues 35 to 38, 59 to 67, and 96 to 101, which are brought together on one

face of the native cyt c structure to form a single contiguous surface.

Residues in the region 36 to 38 have not previously been identified as part of the E8 epitope. The present results strongly implicate this region as part of the binding site for several reasons. These residues are selectively slowed in the complex with protection factors near the theoretically expected limit (see Table 1), are sequentially adjacent, and are spatially adjacent to others that have been clearly identified by other methodologies to be in the E8 epitope (residues 59; 60, and 66) (4, 5, 14).

The 20-fold slower exchange rate observed for the Gln<sup>12</sup> NH in the bound form (Table 1) is puzzling because it is located on a face of the antigen opposite to the surface on which the other 11 residues lie, and neighboring residues in the amino-terminal helix of cyt c are not slowed by binding to E8 (see Table 1 and compare Gln<sup>12</sup> and Cys<sup>14</sup> in Fig. 2). We do not believe, therefore, that Gln<sup>12</sup> is part of the epitope recognized by E8; this remote slowing effect will require some other explanation. An error in the resonance assignment is unlikely since it is based on unambiguous NOE connectivities in the amino-terminal helix that were confirmed under several different solvent conditions (16).

In considering the observed range of protection factors for cyt c, it is useful to examine two limiting cases.

1) If the exchange reaction is mediated by very local structural fluctuations (such as the breakage of an individual hydrogen bond), only amide groups directly involved in the antibody binding site would be shielded in the complex and display large protection

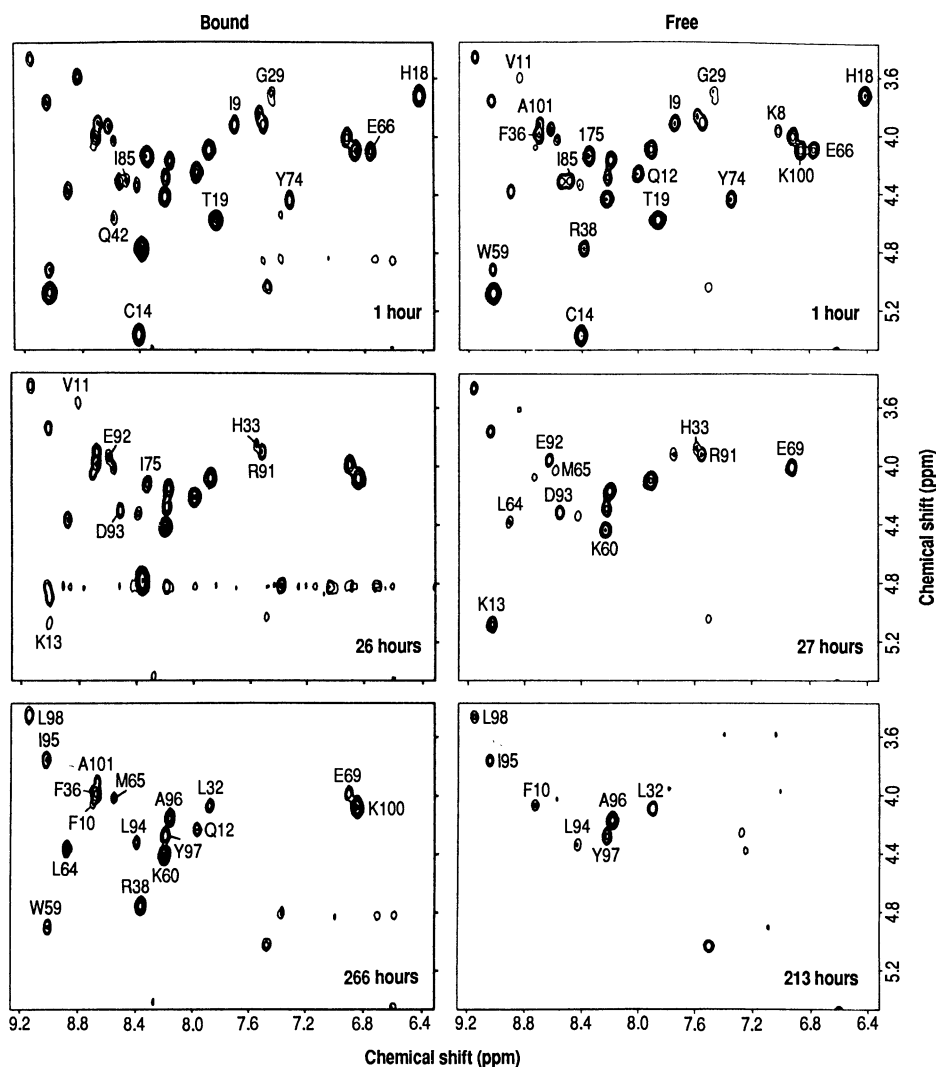


**Fig. 2.** Sections of 2D NMR spectra of representative cyt c samples after partial H-D exchange in the presence (**left**) and absence (**right**) of the E8 MAb. Exchange experiments were carried out with samples in the oxidized form following the procedures described in Fig. 1 for the antibody-bound samples. The NMR spectra were then recorded at 20°C on  $\sim 1.5$  mM samples of reduced cyt c in D<sub>2</sub>O at pD 5.3. Expanded contour plots containing most of the NH-C $\alpha$ H cross peaks are shown for 2D *J*-correlated spectra (COSY) recorded in the magnitude mode (26) at 500 MHz on a Bruker AM 500 spectrometer. Cross peaks are labeled with the assignments reported by Wand *et al.* (16, 27). Four additional cross peaks from slowly exchanging amide protons (residues 7, 68, 70, and 99) lie outside the spectral region shown. A spectral width of 9090 Hz was used in both dimensions; 128 transients of 1024 complex data points were recorded for each of 400  $t_1$  increments. The data were processed on a MicroVAX II computer with the program FTNMR (courtesy of Hare Research, Woodinville, Washington). Unshifted sine multiplication and 3-Hz line-broadening were applied in each dimension prior to Fourier transformation. The final digital resolution was 8.9 Hz in both dimensions. Cross-peak volumes were determined by volume integration with a three-point radius for resolved peaks and a two-point radius in crowded areas. The average volume of three cross peaks from nonlabile protons was used as an internal intensity standard to normalize the data between spectra.

factors, while more peripheral amide protons would exchange essentially at the rate of the free antigen. In this case, the boundaries of the epitope would be clearly defined by a sharp decrease in protection factors. For amide protons that exchange relatively rapidly in the free antigen, the local mechanism with exchange through small low-energy structural fluctuations can be expected to dominate.

2) If the exchange event involves cooperative unfolding of more extensive regions, all of the amide protons involved in a cooperative unit may experience similar retardation upon binding. Residues not directly involved in the binding site might then also be affected. More slowly exchanging protons may, in general, reflect more global, cooperative structural unfolding. It may therefore be most

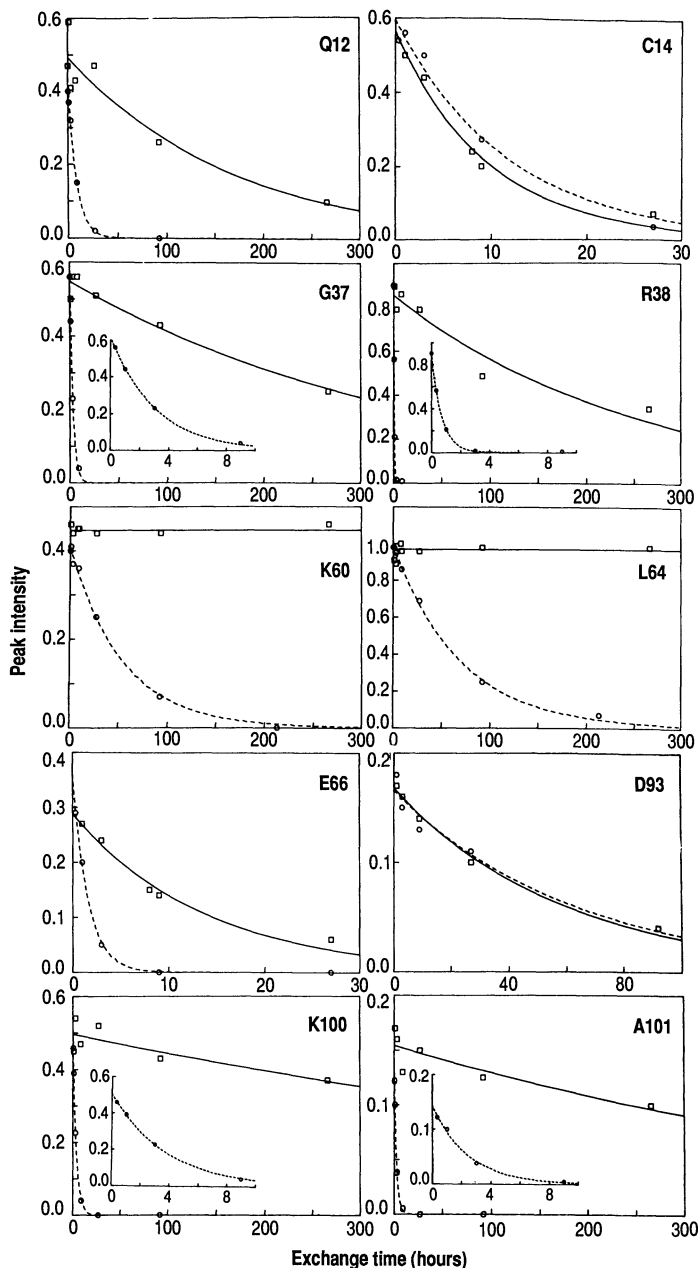


**Fig. 3.** Effect of antibody binding on the kinetics of H-D exchange for some amide protons in horse cyt c. The normalized intensity for resolved NH-C $\alpha$ H cross peaks in COSY spectra (see Fig. 2) is plotted as a function of the H-exchange time in the bound form ( $\square$ , solid lines) and in the free form ( $\circ$ , dashed lines). The data for free oxidized cyt c were obtained from earlier H-exchange studies (18, 28). The curves are exponential fits determined by nonlinear least-squares analysis.

**Table 1.** Effects on ferricytochrome c H-exchange due to binding of the E8 MAAb. Residues with protection factors greater than 3 are listed. Residues with measurable exchange rates in both the free and the bound form, and with  $k_{\text{free}}/k_{\text{bound}}$  of 0.5 to 3, are as follows: Lys<sup>7</sup> ( $k_{\text{free}}/k_{\text{bound}} = 2.6$ ), Lys<sup>8</sup> (1), Ile<sup>9</sup> (0.5), Val<sup>11</sup> (0.5), Lys<sup>13</sup> (0.7), Cys<sup>14</sup> (0.9), Ala<sup>15</sup> (0.6), His<sup>18</sup> (1.0), Thr<sup>19</sup> (0.9), Gly<sup>29</sup> (1.1), Leu<sup>32</sup> (0.9), His<sup>33</sup> (0.9), Gln<sup>42</sup> (~3), Glu<sup>69</sup> (3.0), Asn<sup>70</sup> (1), Tyr<sup>74</sup> (1.8), Ile<sup>75</sup> (2.2), Ile<sup>85</sup> (1), Arg<sup>91</sup> (0.9), Glu<sup>92</sup> (0.7), and Asp<sup>93</sup> (1.1). The effect of antibody binding could not be determined for Phe<sup>10</sup>, Leu<sup>68</sup>, and Leu<sup>94</sup> through Lys<sup>99</sup> because their exchange rates were too slow to measure even in free cyt c. For the remaining 60 non-proline residues, exchange is too fast for 2D NMR analysis under the conditions used in both free ferricytochrome c and the E8 complex. Hydrogen-bond acceptors are the main-chain carbonyl O atoms except for Lys<sup>60</sup>, the acceptor for which is the O $\gamma$  atom of the Thr<sup>63</sup> side chain (16). Statistical errors in individual exchange rates, which depend on the signal-to-noise ratio of the COSY cross peaks, degree of exchange covered, and other experimental variables, are between about 2 and 15%. The true experimental errors depend also on other factors that were difficult to quantitate, such as pH variation, cross-peak overlap, and  $t_1$  noise.

| Residue            | Hydrogen-bond acceptor | $k_{\text{free}}$ (hour <sup>-1</sup> ) | $k_{\text{bound}}$ (hour <sup>-1</sup> ) | $k_{\text{free}}/k_{\text{bound}}$ |
|--------------------|------------------------|---|--|------------------------------------|
| Gln <sup>12</sup>  | Lys <sup>8</sup>       | 0.12                                    | 0.006                                    | 20                                 |
| Phe <sup>36</sup>  | H <sub>2</sub> O       | 0.074                                   | <0.001                                   | >75                                |
| Gly <sup>37</sup>  | Trp <sup>59</sup>      | 0.33                                    | 0.0028                                   | 120                                |
| Arg <sup>38</sup>  | Leu <sup>35</sup>      | 1.44                                    | 0.0042                                   | 340                                |
| Trp <sup>59</sup>  | Arg <sup>38</sup>      | 0.065                                   | <0.0005                                  | >130                               |
| Lys <sup>60</sup>  | Thr <sup>63</sup>      | 0.018                                   | <0.0003                                  | >60                                |
| Leu <sup>64</sup>  | Lys <sup>60</sup>      | 0.014                                   | <0.0003                                  | >50                                |
| Met <sup>65</sup>  | Lys <sup>61</sup>      | 0.004                                   | <0.0005                                  | >10                                |
| Glu <sup>66</sup>  | Glu <sup>62</sup>      | 0.62                                    | 0.073                                    | 8                                  |
| Tyr <sup>67</sup>  | Thr <sup>63</sup>      | 0.04                                    | 0.0058                                   | 7                                  |
| Lys <sup>100</sup> | Ala <sup>96</sup>      | 0.27                                    | 0.0011                                   | 250                                |
| Ala <sup>101</sup> | Tyr <sup>97</sup>      | 0.41                                    | 0.0018                                   | 230                                |

useful to focus on amide protons with large protection factors and relatively rapid exchange rates in the free form, since these are more likely to exchange by way of small fluctuations and provide the most accurate structural definition of the binding site. The residues listed in Table 1 fall into this category.

For most of the NH groups measured in this study, global cooperativity can be ruled out, since their exchange rate is insensitive to antibody binding and there is a relatively sharp distinction between affected residues (protection factors  $\geq 7$ ) (Table 1) and those that are not affected (protection factors  $\leq 3$ ). However, cooperative effects may play a role for the helical region from residue 60 to 70. The residues in the amino-terminal half of the helix (60 to 65) show strong protection (Table 1), while the residues toward the carboxyl-terminal end (residues 66, 67, 69, and 70) display decreasing protection factors (8, 7, 3, and 1, respectively). This pattern suggests that the binding site includes the exposed first turn of the helix (60 to 64), while the carboxyl-terminal end (66 to 70) may lie at the edge of the epitope and exchange through local unwinding from the carboxyl-terminus of the helix, even in the antibody-bound state.

Exchange of a hydrogen-bonded NH can be mediated by motions of the hydrogen-bond donor or acceptor, or both, and complete protection against exchange in the antibody complex may require stabilization of both residues involved in the hydrogen bond. Selective stabilization of one hydrogen-bond partner, perhaps at the edge of the binding site, is thus another potential source of variation in the apparent protection factors.

**Three discontinuous regions form the antigenic site.** The hydrogen exchange results are consistent with the results of previous epitope mapping studies (4-6, 17, 25). Chemical modification experiments and comparison with a homologous cyt c have indicated that the side chains of Trp<sup>59</sup> and Lys<sup>60</sup> play an important role in the affinity of E8 for horse cyt c (4, 17, 25) and that Glu<sup>66</sup> makes a

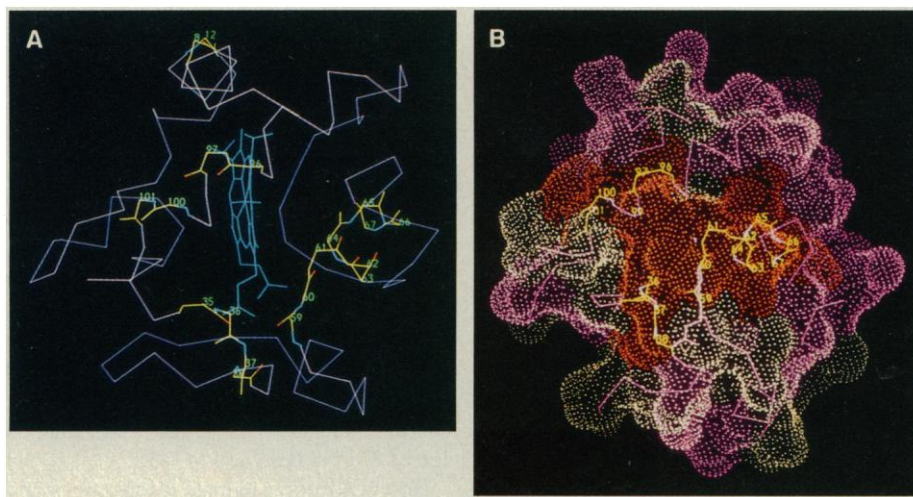


**Fig. 4.** Computer graphics representations of the E8 epitope on horse cyt c (29). (A) The  $\alpha$ -carbon backbone of horse cyt c is shown in violet, the main chain of the residues identified in Table 1 of this study and their hydrogen-bond acceptors are shown in yellow, and the amide hydrogen-donor and carbonyl group hydrogen-bond acceptor are shown in blue and red, respectively. (B) A surface view of the epitope with the residues protected from hydrogen exchange identified in this study (excluding Gln<sup>12</sup>) and their hydrogen-bond acceptors shown in orange (that is, 35 to 38, 59 to 67, 96, 97, 100, and 101). Also shown in orange is residue 99 identified previously (25). Residues that are thought not to be part of the epitope from this study (3 to 5, 7 to 11, 13 to 15, 17 to 19, 29, 31 to 33, 68 to 71, 74, 75, 85, 87 to 89, and 91 to 93) and from a previous study (25) (8, 22, 25, 27, 39, 53, 55, 72, 73, 79, 86, and the  $\epsilon$  atoms of 99) are colored magenta. Residues not yet identified are shown in gray.

lesser but still significant contribution (5). Another residue, Lys<sup>99</sup>, which was protected in acetylation experiments (25), is located in the carboxyl-terminal helix. Neighboring residues Lys<sup>100</sup> and Ala<sup>101</sup> have NH exchange rates reduced by greater than 200-fold in the antibody bound form (Table 1). The  $\epsilon$ -amino group of Lys<sup>100</sup> was not protected in the prior acetylation experiments (25), presumably because the Lys side chain can extend far (12 Å) from the backbone amide group measured here. Since the exchange of the amide protons of Lys<sup>99</sup> and the adjacent residues, 94 to 98, in the carboxyl-terminal helix, was too slow to measure in these experiments, it is still unclear if these residues are involved in the epitope. However, hydrogen exchange of three residues in the next helix turn (91 to 93) was insensitive to antibody binding, indicating that the epitope is limited to the structurally more exposed carboxyl-terminal end of the helix.

The present results place the E8 epitope on horse cyt c as shown in Fig. 4, although they do not specify that all of these residues individually bind the antibody site. In Fig. 4A only the polypeptide backbone atoms and the protected amide protons and hydrogen-bond acceptors defined in this study are displayed. The greatest linear extent of the epitope, measured as a C $\alpha$ -C $\alpha$  interatomic distance, is  $\sim$ 20 Å. The space-filling representation in Fig. 4B shows in orange the total surface area mapped out by the side chains of the protected residues, other than Gln<sup>12</sup> and the  $\epsilon$  atoms of the side chain of Lys<sup>100</sup>, which are excluded for the reasons discussed. Residues known from this, and previous studies (25), not to be part of the epitope are shown in magenta, and as yet unidentified residues are shown in gray. The summed water-accessible surface area, for the three regions of the polypeptide chain of horse cyt c buried by interaction with E8, is about 750 Å<sup>2</sup> (shown in Fig. 4B in red). These findings are consistent with crystallographically determined epitopes on lysozyme recognized by three monoclonal antibodies that are similar in size and also involve residues from several discontinuous segments of the polypeptide chain (1, 2).

#### REFERENCES AND NOTES

1. A. G. Amit, R. A. Mariuzza, S. E. V. Phillips, R. J. Poljak, *Science* **233**, 747 (1986); S. Sheriff *et al.*, *Proc. Natl. Acad. Sci. U.S.A.* **84**, 8075 (1987); P. M. Colman, *Adv. Immunol.* **43**, 99 (1988).
2. D. R. Davies, S. Sheriff, E. A. Padlan, *J. Biol. Chem.* **263**, 10,541 (1988).
3. D. C. Benjamin *et al.*, *Annu. Rev. Immunol.* **2**, 67 (1984); R. Jemmerson and Y.

4. H. M. Cooper *et al.*, *J. Biol. Chem.* **262**, 11,591 (1987).
5. J. F. Collawn, C. J. A. Wallace, A. E. I. Proudfoot, Y. Paterson, *ibid.* **263**, 8625 (1988).
6. R. Jemmerson and Y. Paterson, *Science* **232**, 1001 (1986).
7. A. Burnens, S. Demotz, G. Corradin, H. Binz, H. R. Bosshard, *ibid.* **235**, 780 (1987).
8. Y. Paterson, in *The Immune Responses to Structurally Defined Proteins: The Lysozyme Model*, S. Smith-Gill and E. E. Sercarz, Eds. (Adenine, Schenectady, NY, 1989), pp. 177-189.
9. R. R. Ernst, G. Bodenhausen, A. Wokaun, *Principles of Nuclear Magnetic Resonance in One and Two Dimensions* (Oxford Univ. Press, Oxford, 1987).
10. K. Wüthrich, *NMR of Proteins and Nucleic Acids* (Wiley, New York, 1986); *Science* **243**, 45 (1989); J. L. Markley, *Methods Enzymol.* **176**, 12 (1989).
11. J. Anglister *et al.*, *Biochemistry* **26**, 6058 (1987).
12. J. Anglister *et al.*, *ibid.* **27**, 717 (1988); J. Anglister, R. Levy, T. Scherf, *ibid.* **28**, 3360 (1989).
13. D. A. Kooistra and J. H. Richards, *ibid.* **17**, 345 (1978); A. M. Goetze and J. H. Richards, *ibid.*, p. 1733.
14. T. Takano and R. E. Dickerson, *J. Mol. Biol.* **153**, 79 (1981); *ibid.*, p. 95.
15. G. W. Bushnell, G. V. Louie, G. D. Brayer, *ibid.*, in press.
16. A. J. Wand and S. W. Englander, *Biochemistry* **25**, 1100 (1986); A. J. Wand, D. L. DiStefano, Y. Feng, H. Roder, S. W. Englander, *ibid.* **28**, 186 (1989); Y. Feng, H. Roder, S. W. Englander, A. J. Wand, D. L. DiStefano, *ibid.*, p. 195.
17. F. R. Carbone and Y. Paterson, *J. Immunol.* **135**, 2609 (1985).
18. A. J. Wand, H. Roder, S. W. Englander, *Biochemistry* **25**, 1107 (1986).
19. J. J. Englander and S. W. Englander, *ibid.* **26**, 1846 (1987).
20. S. W. Englander and N. R. Kallenbach, *Q. Rev. Biophys.* **16**, 521 (1984).
21. P. Brandt and C. Woodward, *Biochemistry* **26**, 3156 (1987).
22. S. W. Englander, *Ann. N.Y. Acad. Sci.* **244**, 10 (1975).
23. C. Woodward, I. Simon, E. Tüchsen, *Mol. Cell. Biochem.* **48**, 135 (1982).
24. G. Wagner and K. Wüthrich, *J. Mol. Biol.* **160**, 343 (1982); K. Kuwajima and R. L. Baldwin, *ibid.* **169**, 299 (1983); G. Louie, J. J. Englander, S. W. Englander, *ibid.* **210**, 765 (1988).
25. M. Oertl, K. Immergluck, Y. Paterson, H. R. Bosshard, *Eur. J. Biochem.* **182**, 699 (1989).
26. W. P. Aue, E. Bartholdi, R. R. Ernst, *J. Chem. Phys.* **64**, 2229 (1976); K. Nagayama, A. Kumar, K. Wüthrich, R. R. Ernst, *J. Magn. Reson.* **40**, 321 (1980).
27. Abbreviations for the amino acid residues are: A, Ala; C, Cys; D, Asp; E, Glu; F, Phe; G, Gly; H, His; I, Ile; K, Lys; L, Leu; M, Met; N, Asn; P, Pro; Q, Gln; R, Arg; S, Ser; T, Thr; V, Val; W, Trp; and Y, Tyr.
28. H. Roder, A. J. Wand, S. W. Englander, unpublished results.
29. Computer graphics representations were constructed with the programs GRAMPS [M. L. Connolly and A. J. Olsen, *Comput. Chem.* **9**, 1 (1985)] and GRANNY [T. J. O'Donnell and A. J. Olsen, *Comput. Graphics* **15**, 133 (1981)] from horse cyt c coordinates. The latter were derived with the use of molecular dynamics calculations by J. Sayre and J. Tainer from the tuna cyt c coordinates determined by Takano and Dickerson (14).
30. We thank J. Englander and P. Emanuel for technical assistance and J. Tainer for preparation of Fig. 4. Supported by the W. W. Smith Charitable Trust, the University of Pennsylvania Research Foundation and BRSO grant S07-RR-05415-28 to Y.P., and NIH grants GM 31847 to S.W.E. and GM 35926 to H.R.

12 April 1990; accepted 16 July 1990